JOURNAL OF NANO- AND ELECTRONIC PHYSICS
Vol. **7** No 1, 01023(7pp) (2015)

ЖУРНАЛ НАНО- ТА ЕЛЕКТРОННОЇ ФІЗИКИ
Том **7** № 1, 01023(7cc) (2015)

Synthesis and Study of the Properties of Nanoferrites Obtained by the Sol-gel Method with Participation of Auto-combustion

V.S. Bushkova*

Vasyl Stefanyk Pre-Carpathian National University, 57, Shevchenko Str., 76025 Ivano-Frankivsk, Ukraine

(Received 17 October 2014; published online 25 March 2015)

The aim of the present work was to create and study ferrite nanocrystalline materials of the system $(ZnxMg1-x)_{1-y}Fe_{2+2y/3}O_4$ with spinel structure using sol-gel technology with participation of auto-combustion. This method is a cheap and low-temperature technique that allows for the fine control on the product's chemical composition. It was found physical and chemical processes and mechanisms of combustion, which take place in the synthesis of ferrites using this technology. It was shown that the process of the dry gel auto-combustion the resulting exothermic reaction at a temperature of about 483 K occurred, due to the interaction of carboxyl groups and NO_3^- ions. It was revealed that the synthesized powders were agglomerated. The thermal analysis of ferrite nanopowders was performed using the DTA technique. The results obtained that elimination of small pores between the crystallites or particles of the agglomerates occurs at the heating. It was shown that in the samples peculiarities in transitions of iron cations in octahedral crystallographic position occur, that affects the degree of reversibility of spinel and leads to a weakening of antiferromagnetic interactions between the *A*-and *B*-sublattice. The role of zinc concentration of the Mg-Zn ferrite samples in the FMR absorption curves was determined and analyzed.

Keywords: Ferrite, Nanocrystalline powders, Sol-gel technology, Thermal analysis, Cation distribution, Mössbauer spectra, FMR-parameters.

PACS numbers: 75.50.Tt, 61.05.cf, 75.75.Fk

1. INTRODUCTION

Currently, soft magnetic ferrites which are compounds of ferric oxide with oxides of other metals take an important place among ferromagnetic materials. Ferrites, as a rule, possess high electrical resistance and, as a consequence, small energy losses during remagnetization. They are the base of many important devices of microwave engineering, computer science and radio electronics [1].

Structure of a ferrite spinel represents a dense cubic face-centered packing of oxygen ions with filling by iron ions and bivalent metal of 1/8 of all tetrahedral (*A*) and 1/2 octahedral (*B*) pores [2]. Magnesium-zinc ferrites [3-7], which are technologically important materials when they are used as magnetic cores on the radio frequencies, take a special place among ferrites with the spinel structure [8]. They are also of great scientific interest in the field of magnetism of complex crystals. Their magnetoelectronic structure determines the magnetic and electrical properties. Unlike many other ferrites with the spinel structure, magnetic properties of Mg-Zn ferrites, which are conditioned by the presence of only one magnetic Fe^{3+} ion [9], depend on the distribution of magnetic atoms over two crystallographic non-equivalent positions with tetrahedral and octahedral environment by oxygen anions of metal ions. Because of the fact that the specified materials are assigned to the non-compensated antiferromagnets, directions of the magnetic moments in Mg-Zn sublattices are mutually opposite.

It is known that choice of the corresponding synthesis process is the key factor to obtain ferrites of high quality [10]. Structure [11], dielectric [12] and magnetic [13] properties of magnesium-zinc ferrites obtained at very high temperatures are well studied to date. A deviation from stoichiometry is often observed if use ceramic processing to obtain Mg-Zn ferrites [14-15].

A tendency to magnetic nanomaterials technology has appeared recently. It is shown in [16] that particles' size influences the distribution of cations over ferrite Ni-Zn sublattices that, in turn, influences their magnetic properties. Nanocrystalline Mg-Zn ferrites are characterized by the size effects [17]. In particles, whose sizes are comparable with the interatomic distances and surface plays the major role, magnetic structure requires a detailed study. Moreover, it was interesting to ascertain how the production technology and chemical composition influence the stoichiometry of the samples of the system $(Zn_xMg_{1-x})_{1-y}Fe_{2+2y/3}O_4$, where y is the stoichiometry index. It is known that ferromagnetic resonance (FMR) line width is an important parameter of ferrites in the microwave band [18]. Thus, since physical properties of Mg-Zn ferrites depend not only on the particles' size, but also on the technique of their synthesis, the aim of the present work is the synthesis, structural, thermal and magnetic investigations of magnesium-zinc ferrite nanopowders obtained by the sol-gel method with participation of auto-combustion.

2. DESCRIPTION OF THE OBJECTS AND METHODS OF RESEARCH

2.1 Synthesis of magnesium-zinc ferrites

The most widespread production technologies of oxide materials are the methods of deposition or mixing of the corresponding components with the subsequent stages of thermal treatment, as a rule, embarrassing to obtain the single-phase products from binary and more complex systems. A great attention is currently devoted to the sol-gel methods among the production technologies of nanomaterials.

* bushkovavira@rambler.ru

Ferrites of the $(Zn_xMg_{1-x})_{1-y}Fe_{2+2y/3}O_4$ system (see Table 1) were synthesized by the sol-gel method with participation of auto-combustion [19] which is the variety of sol-gel synthesis techniques of the chemically modified materials which has found a wide application in practice now. This method is rather simple and it does not require any complicated and expensive equipment, therefore, it is one of the most promising production technologies of nanomaterials that allows to synthesize complex oxide systems including ferrite powders of different chemical compositions for magnetic devices and nodes of electronic engineering.

Table 1 – Formula of ferrite powders

x	*y*	Formula
0.0	0.0	$MgFe_2O_4$
0.2	0.0	$Zn_{0.2}Mg_{0.8}Fe_2O_4$
0.44	0.05	$Zn_{0.42}Mg_{0.53}Fe_{2.03}O_4$
0.44	0.0	$Zn_{0.44}Mg_{0.56}Fe_2O_4$
0.44	– 0.05	$Zn_{0.46}Mg_{0.59}Fe_{1.97}O_4$
0.5	0.0	$Zn_{0.5}Mg_{0.5}Fe_2O_4$
0.55	0.0	$Zn_{0.55}Mg_{0.45}Fe_2O_4$
0.6	0.0	$Zn_{0.6}Mg_{0.4}Fe_2O_4$

From the point of view of the power inputs, sol-gel method with participation of auto-combustion compared with the ceramic one is a cost efficient production technology of the complex oxide systems [20]. The idea of the method is to use the exothermic reaction heat in the synthesis of powders. In a number of cases, this process, namely, the use of the exothermic reaction heat to maintain the reaction, is steadily developed, i.e. a narrow combustion zone, in which, in fact, the reaction occurs, passes over the sample. The procedure of this method consists in the synthesis of the materials with the specified physical and chemical properties including the production of the sol and its successive transformation into the gel. For example, 0.01 mole of magnesium nitrate, 0.02 mole of ferric nitrate and 0.03 mole of citric acid in the ratio of molar masses of the metal nitrates in citric acid of 1 : 1 are used in the synthesis of $MgFe_2O_4$ in order to obtain the sol. Presence of citric acid is explained as follows: formation of the nitrate-citrate complexes of metals eliminates the difference in the individual behavior of cations in the solution [21] that promotes a more complete mixing and allows to avoid separation of the components in the further stages of the synthesis. Distillated water was used as the dispersion phase. Hydrolysis reactions leading to the formation of the sol, in which particles of metal hydroxides (whose size does not exceed a few nanometers) serve as the dispersion phase, occur during mixing of precursors:

$$Mg(NO_3)_2 + 2H_2O \rightarrow Mg(OH)_2 + 2HNO_3, \quad (1)$$

$$Fe(NO_3)_2 + 3H_2O \rightarrow Fe(OH)_3 + 3HNO_3. \quad (2)$$

Neutralization reaction of the dispersion medium [22] takes place upon addition of NH_4O to the obtained colloidal solution

$$NH_4OH + HNO_3 \rightarrow NH_4NO_3 + H_2O + 145 \text{ kJ/mole}. \quad (3)$$

Neutralization of the dispersion medium using 25 % aqueous ammonia to the level of pH = 7, in turn, leads to the intense formation of aggregates of particles. To provide the gel-formation process, in this case, energy injection to the reaction system is necessary even if the neutralization reaction is exothermic one. Increase in the concentration of the dispersion phase results in the initiation of the coagulation contacts between particles and beginning of the structuring, i.e. formation of the monolithic gel in which molecules of solvent (water) are in the flexible, but rather stable three-dimensional network, which is formed of the particles of hydroxides. Moreover, injection of additional energy is required for the subsequent drying of the gel in order to transform it into the xerogel due to evaporation of the dispersion medium. During drying, xerogel spontaneously catches fire with the formation of a single-phase ferrite with the spinel structure and combustion products. Auto-combustion occurs as follows: ammonia water in combination with nitric acid (generated in the hydrolysis reaction) forms ammonium nitrate (NH_4NO_3) and water. At the end of the evaporation process of the dispersion medium at the temperature of about 483 K, decomposition of the ammonium nitrate with release of heat of 38 kJ/mole takes place. Effect of the ferrite formation from metal oxides also promotes the combustion process:

$$MgO + Fe_2O_3 \rightarrow MgFe_2O_4 + 20 \text{ kJ/mole}. \quad (4)$$

The confirmation of this at the temperature of about 483 K is the exothermic peak on the differential-thermal curve (see Fig. 1) which indicates that dry gel formed of metal nitrates and citric acid is burned during the auto-combustion process which propagates rapidly until xerogel is burned down, resulting in the formation, in this case, a friable nanodispersed powder. Change in the xerogel mass is approximately equal to 75 %.

Thermally induced anion oxidation-reduction reaction promotes the combustion process of the dry gel [23]. Due to this reaction, a sufficient amount of energy is released for the formation of the ferrite phase in a very short time. Because of the auto-combustion of xerogel, organic residues, i.e. citric acid, are burned out. Power inputs during initiation of the auto-combustion reaction are significantly less than those which are necessary to perform a long-term high-temperature annealing during ceramic synthesis.

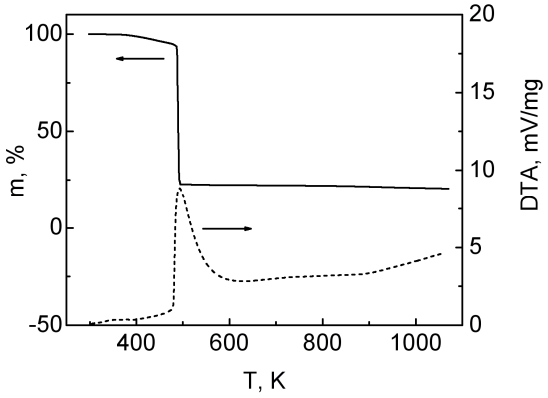

Fig. 1 – DTA-TG curves of the $MgFe_2O_4$ xerogel

2.2 Research methods

Phase composition was controlled by X-ray structural analysis performed on the diffractometer DRON-3 using Cu(Kα)-radiation. Morphology of the powders was investigated by the scanning electron microscope NeoScope JSM-5000 by JEOL.

Thermal analysis of the samples was carried out by the synchronous thermal analyzer STA 449 F3 Jupiter in linear heating mode with the rate of 10 K/min in the temperature range of 298-1073 K that resulted in the experimentally obtained curves of the thermogravimetric (TG) and differential thermal analysis (DTA). Mass change upon heating was determined with the accuracy of 10^{-6} kg.

Mössbauer absorption spectra of magnesium-zinc samples are obtained at room temperature using spectrometer MS-1104Em. ^{57}Co of the activity of 100 mCi in a chromic matrix was used as the source of γ-quanta. The scintillation counter, in which crystal NaI served as the sensing element, was used for the detection of γ-quanta. Decomposition of the experimental Mössbauer spectra into the components is performed using the universal program "Univem MS"-2.07 by approximation by the sum of analytical functions describing separate components of the experimental spectrum.

FMR spectra were detected at room temperature by the modernized commercial spectrometer SE/X-2013. The obtained FMR spectra were analyzed using the programs "Origin 7" and "SimFonia" by Bruker.

3. DESCRIPTION AND ANALYSIS OF THE RESULTS

3.1 Phase analysis and particles' size of the obtained powders

According to the performed analysis, experimental X-ray diffraction patterns of the samples (Fig. 2) obtained by the sol-gel method with participation of auto-combustion indicate the cubic spinel structure of the spatial Fd3m group. This implies that ferrites are directly formed after auto-combustion of xerogel.

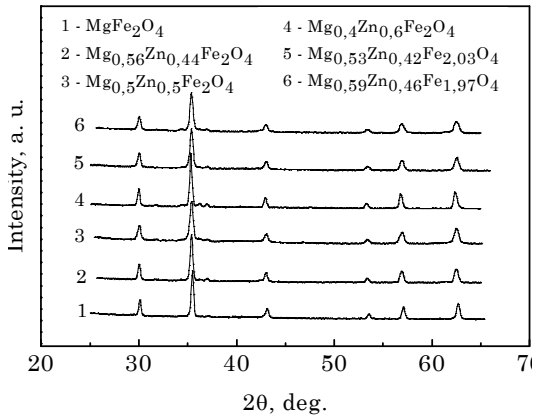

Fig. 2 – Diffraction patterns of the $(Zn_xMg_{1-x})_{1-y}Fe_{2+2y/3}O_4$ system

As seen from the X-ray diffraction patterns of magnesium-zinc samples, they all are almost single-phase. When substituting Mg^{2+} ions for Zn^{2+} ions, one observes the presence of the zinc oxide phase, amount of which increases with increasing parameter x in the system. The maximum content of the ZnO phase, which accounts for 3 % of the total composition, is observed for the sample $Mg_{0.4}Zn_{0.6}Fe_2O_4$.

The average diameter of particles of magnesium-zinc powders is established using the Scherrer formula:

$$\langle D \rangle = \frac{0.9\lambda}{\beta \cdot \cos\theta}, \quad (5)$$

where β is the integral width of the diffraction reflex, broadening of which is conditioned by the influence of the sample dispersivity; λ is the X-ray radiation wavelength; θ is the angle between the diffracted and incident rays. Particles' size according to the peak (222) is about equal to 20-35 nm.

Micrograph of the magnesium-zinc powder (Fig. 3) confirms the above statements. Comparison of the crystallite size according to the results of the X-ray analysis and scanning electron microscopy indicates that ferrite powders obtained by the sol-gel method with participation of auto-combustion form agglomerates.

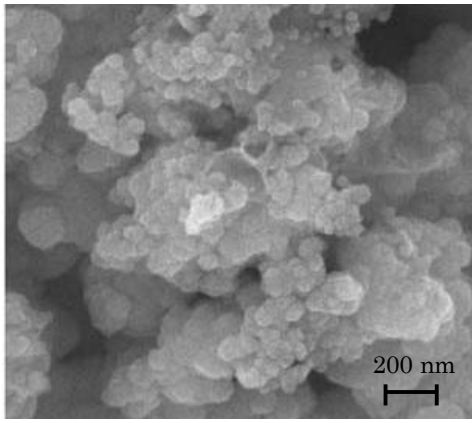

Fig. 3 – Morphology of the $Mg_{0.5}Zn_{0.5}Fe_2O_4$ powder

Depending on the degree of diamagnetic substitution, parameters of the crystal structure of the studied samples are calculated (see Table 2). The values of the lattice constant a and X-ray density d_x are obtained by the following formulas:

$$a = \frac{\lambda}{2\sin\theta}\sqrt{h^2 + k^2 + l^2}, \quad (6)$$

θ are the angles, at which the peaks were observed; h, k, and l are the Miller indexes;

$$d_x = 8M/N_a a^3, \quad (7)$$

where M is the molar mass of the sample; N_a is the Avogadro constant.

Table 2 – Dependence of the lattice constant and X-ray density on the composition of the samples

$Mg_{1-x}Zn_xFe_2O_4$		
x	a, nm	d_x, kg/m^3
0.0	0.8383	4.51
0.2	0.8383	4.69
0.44	0.8406	4.88
0.5	0.8406	4.93
0.55	0.8407	4.98
0.6	0.8416	5.01

It was of interest to determine in ferrites of the stoichiometric composition by the X-ray diffraction method the cation distribution over sublattices in the structure of ferrites using the dependence of the integral intensities of diffraction lines from the position of atoms in the unit cell and their atomic number.

As known, for the materials with the spinel structure reflections from the planes (220) and (422) correspond to the diffraction on the tetrahedral cations and reflections from the plane (222) – on the octahedral ones. I_{220}/I_{400} intensities ratio is sensitive to the change in the cation distribution and I_{111}/I_{400} ratio – to the change in the oxygen parameter.

Magnesium-zinc ferrites belong to the mixed ferrites which, besides Fe^{3+} ions, contain two other sorts of cations with the tendency to occupy the same holes of the crystal lattice which they would occupy in the corresponding monoferrites. For example, in the mixed ferrites with the normal spinel structure, namely $Zn_xCd_{1-x}Fe_2O_4$, Zn^{2+} and Cd^{2+} cations occupy the tetrahedral holes, while Fe^{3+} cations are located in the octahedral spaces. If solid solutions of two ferrites have the reversed spinel structure, then a half of cations is located in the tetrahedral holes and the other half and the rest, typical for the specified spinel, of cations – in the octahedral holes. The situation should not be changed even for the case when solid solutions consist of the normal and reversed spinels. Thus, if Zn^{2+} or Cd^{2+} ions will enter the composition of the mixed spinel, they will occupy the tetrahedral spaces, and Mg^{2+}, Ni^{2+}, Co^{2+} ions and others – the octahedral ones. With increasing concentration of the normal structure spinel, amount of Fe^{3+} caions in tetra-holes decreases, respectively. The latter are displaced by Zn^{2+} and Cd^{2+} cations into the octahedral spaces. However, depending on the method and conditions for producing, some deviations from the above rules are possible. It is known [24] that Mg^{2+} and Ni^{2+} cations contained in the mixed ferrites can occupy both the octa- and tetra-positions after rapid cooling.

Composition and structure of the ferro-spinel with a glance to the cation distribution over the crystallographic positions can be described by the structurally-chemical formula $Mg_{1-x-l}Zn_xFe_l[Mg_lFe_{2-l}]O_4$, where l is the degree of reversibility of the spinel structure; square brackets contain metal atoms located in the octahedral positions and before brackets – in the tetrahedral positions. Since amount of the zinc oxide phase in magnesium-zinc samples is so insignificant, its influence on the cation distribution can be neglected. Taking into consideration this fact, the structural formulas for each of the studied samples are obtained (see Table 3).

Table 3 – Cation distribution in magnesium-zinc ferrites

Degree of substitution, x	Cation distribution of ions over the spinel sublattices
0.0	$(Mg_{0.22}Fe_{0.78})[Mg_{0.78}Fe_{1.22}]O_4$
0.2	$(Mg_{0.21}Zn_{0.20}Fe_{0.59})[Mg_{0.59}Fe_{1.41}]O_4$
0.44	$(Mg_{0.11}Zn_{0.44}Fe_{0.45})[Mg_{0.45}Fe_{1.55}]O_4$
0.5	$(Mg_{0.11}Zn_{0.50}Fe_{0.39})[Mg_{0.39}Fe_{1.61}]O_4$
0.55	$(Mg_{0.08}Zn_{0.55}Fe_{0.37})[Mg_{0.37}Fe_{1.63}]O_4$
0.6	$(Mg_{0.04}Zn_{0.60}Fe_{0.36})[Mg_{0.36}Fe_{1.64}]O_4$

According to the tabular data, an insignificant part of Mg^{2+} cations occupy the position in the tetra-sublattice displacing thus Fe^{3+} cations into the octa-sublattice. As a rule, Zn^{2+} cations tend to be placed in the spinel tetra-sublattice that is confirmed experimentally.

Since sol-gel method with participation of auto-combustion is a little studied technique for production of nanomaterials, it is important to establish the cooling mode of particles after the auto-combustion process based on the data of the cation distribution over sublattices of the magnesium-zinc ferrites.

Since cation distribution of magnesium ferrites is sensitive to the temperature-time mode of the material synthesis, degree of reversibility focusing on the unsubstituted magnesium ferrite correspond to the rapid cooling mode from 1473 K. According to [25], during rapid cooling of the ferrite obtained by the ceramic method, degree of reversibility of the spinel structure is equal to 0.78. During slow cooling of the magnesium ferrite $l \approx 1$. As seen from Table 3, degree of reversibility of the spinel during rapid cooling coincides with its numerical value for the magnesium ferrite obtained by the sol-gel method with participation of auto-combustion. This conclusion is important from the point of view of understanding the kinetics of the processes occurring during such a little studied technique as the sol-gel method with participation of auto-combustion.

3.2 Thermal analysis of the synthesized powders

Since it is difficult to regulate the processes of combustion and thermal synthesis, there is a real possibility to correct the synthesis modes conducting an additional controlled thermal treatment. In order to explain the auto-combustion process of the nitrate-citrate xerogel, the DTA and TG analyses have been performed. It was established in [23] that the process of xerogel combustion can be considered as thermally induced oxidation-reduction reaction, at which the citrate ions act as the reducer and the nitrate ones – as the oxidizer. Due to the presence of NO_3^- ions which provide the decomposition of the organic component, rate of oxidation reaction relatively increases. This results in the release of a sufficient amount of energy for the formation of the ferrite phase in a very short time.

Thus, exothermal peak on the DTA curve (see Fig. 1) corresponds to the oxidation-reduction reaction between the nitric and citrate systems.

DTA of the obtained magnesium-zinc powders has not shown the pronounced intensive in value and short in time thermal effects, therefore, an additional differentiation of the obtained DTA-data has been performed (Fig. 4) that allowed to establish with high precision the start temperature of the thermal effects. Intensive minima correspond to the points of inflection on the thermogram taken by thermal analyzer, when thermocouple on the sample shows the decrease in the temperature compared with the standard, i.e. the endo-effect beginning.

As seen on the temperature dependence of the dE/dT derivative (Fig. 5), heating of the $Mg_{1-x}Zn_xFe_2O_4$ samples to the temperature of about 473 K induces the beginning of the endothermic effect. This effect does not depend on the chemical composition of ferrites and is not accompanied by the mass change. Probably, the specified endo-effect is conditioned by the re-distribution of particles in the powder on account of the destruction of the organic combustion residues.

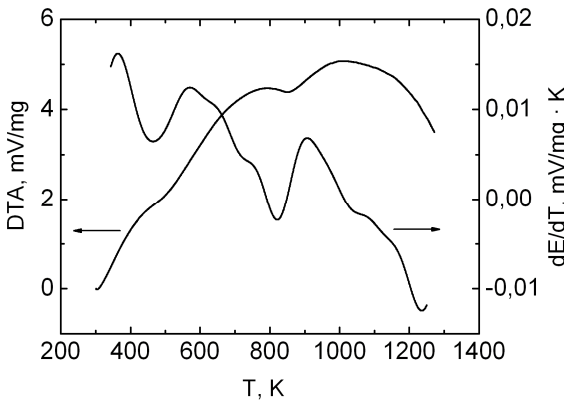

Fig. 4 – Temperature dependence of the DTA-curve and its derivative for the $Mg_{0.4}Zn_{0.6}Fe_2O_4$ sample

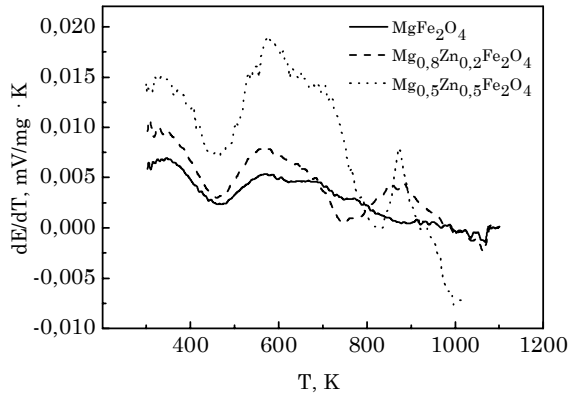

Fig. 5 – Temperature dependence of dE/dT of magnesium-zinc samples

With further heating of the powders to higher temperatures, another effect, which takes a heat, appears. However, in this case, endo-effect significantly depends on the content of Zn^{2+} cations in the composition of the powders (Table 4) and is not almost accompanied by the change in their masses

Table 4 – Influence of the heating temperature of the samples on the beginning of the thermoeffects

Composition, x	1-st endo-effect, K	2-nd endo-effect, K
0.0	468	753
0.2	469	773
0.44	471	803
0.5	468	823
0.55	470	833
0.6	468	848

The second endo-effect, most likely, is associated with the phenomena occurring on the surface of the samples during their heating. Elimination of small pores between crystallites or particles in agglomerates can belong to these phenomena. We should note that the given endo-effect is not connected with the healing of possible point defects in the powders, since the temperature, at which the endo-effect takes place, is substantially lower than the temperature of the diffusion processes in ferrites [26]. As the concentration of Zn^{2+} cations in the composition of the samples increases, the second endo-effect is shifted toward the range of high temperatures (Table 4). Since Zn^{2+} cations are heavier than Mg^{2+} cations, then substitution of Mg^{2+} cations in $Mg_{1-x}Zn_xFe_2O_4$ system leads to the intensification of the agglomeration process of particles into nanoclusters.

3.3 Mössbauer investigations

Since magnetic properties of ferrites significantly depend on the chemical composition and microscopic structure, the microscopic properties of magnesium-zinc samples have been studied. Investigation by the Mössbauer method of the effective magnetic fields, electric field gradients on nuclei of different ions in ferrites and energy shifts of the absorption spectra allows to obtain information about the symmetry of the environment of a separate ion, nature of the transition to the ordered state and electron density on nuclei. Judging by the line intensity of the Mössbauer spectra, it is possible to estimate the relative number of nuclei located in different crystallographic positions.

Line width is the property of the γ-radiation without recoil. If lattice becomes excited with γ-quantum release, then effective width of the γ-line is equal to the phonon energy by the order of magnitude. For the case, when lattice is not excited, width of the phononless radiation component is characterized by only the width of nuclear levels, between which the transition occurs.

Asymmetrical Zeeman pattern is discovered in the Mössbauer absorption spectra of the investigated samples obtained at room temperature (see Fig. 6) that is confirmed by different signs of deviation from the experiment for positive and negative velocities.

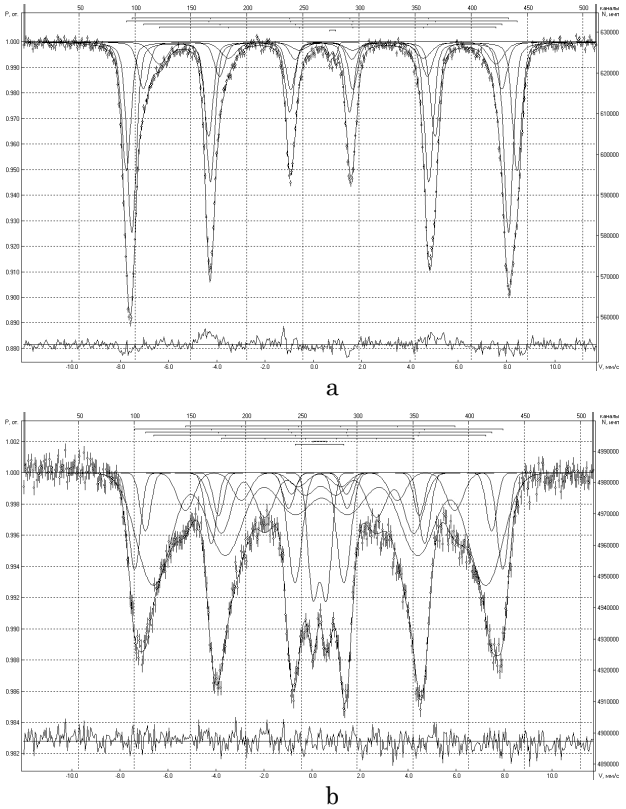

Fig. 6 – Mössbauer spectra of the samples of $MgFe_2O_4$ (a) and $Mg_{0.5}Zn_{0.5}Fe_2O_4$ (b) compositions

Broadening of a magnetic sextuplet is observed with increasing of zinc ions in the composition of magnesium-zinc ferrites. Moreover, intensity of the central quadru-

pole doublet grows along with the increase in the concentration of Zn^{2+} ions. Increase in the paramagnetic doublet intensity is associated with a number of magnetic phenomena, namely, existence of superparamagnetic particles [27] and magnetic phase with noncollinear arrangement of the magnetic moment vectors. In this case, irrespective of the degree of substitution x, presence of the magnetic-ordered phase is clearly observed.

Increase in the Zn^{2+} content in the samples leads to the decrease in the value of the effective magnetic fields in nuclei. Obviously, the decrease in the magnetic fields induces weakening of the *A*-*B* interaction in the spinel structure.

3.4 Features of the ferromagnetic resonance study of nanoferrites

It is known that ferromagnetic resonance frequency depends both the value of the external magnetizing field and the crystallographic anisotropy field, demagnetizing field of the particles shape and possible defects of the samples structure. For the ferrite powders, the FMR-spectra were taken at room temperature and the field dependences of the derivative of the imaginary sensibility on the magnetic induction are shown (Fig. 7).

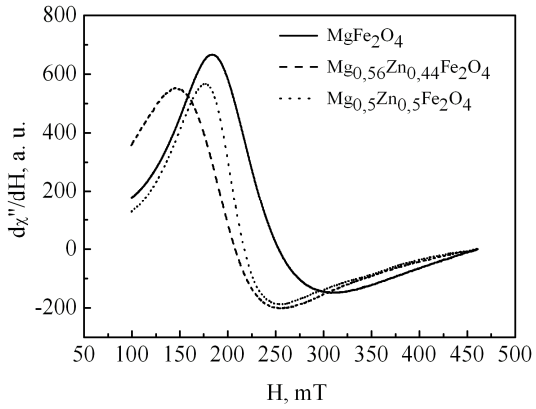

Fig. 7 – FMR-spectra of $Mg_{1-x}Zn_xFe_2O_4$ ferrites

Based on the experimentally obtained FMR-curves, we have calculated the FMR-absorption line width ΔH_{pp}, Landé factor (or *g*-factor) and gyromagnetic ratio γ (see Table 5). Line width ΔH_{pp} is characterized by the distance between the sides of the resonance absorption curve at its half-height.

Table 5 – Parameters of the FMR-signal of the studied nanocrystalline ferrites

x	*g*-factor	γ, 10^{11} (s·T)$^{-1}$	ΔH_{pp}, 10^{-3} T
0.0	2.85 ± 0.02	2.50 ± 0.02	128.0 ± 2
0.44	3.43 ± 0.02	3.02 ± 0.02	101.0 ± 2
0.5	3.20 ± 0.02	2.81 ± 0.02	79.0 ± 2

According to the analysis of the performed experimental study for magnesium-zinc ferrites, FMR line width decreases with increasing concentration of Zn^{2+} ions in the samples composition. Parameters of the FMR-ferrites considerably depend on the magnetic ion components entering each spinel sublattice [28]. In the case of ferrites of the $Mg_{1-x}Zn_xFe_2O_4$ system, only Fe^{3+} ions possess the magnetic moment and which with increasing degree of substitution x tend to occupy the octahedral crystallographic positions that leads to attenuation of the antiferromagnetic interaction between *A*- and *B*-sublattices resulting in the decrease in the FMR line width. Obviously, degree of reversibility of the spinel (which also decreases with the growth of the parameter x) influences the FMR line width.

Thus, experimental data of the FMR-investigation of magnesium-zinc ferrites confirms the results of the cation distribution obtained based on the X-ray structural analysis of the samples.

For ferromagnets, resonance line width is connected with the magnetic relaxation time by the relation

$$\tau = 2/\gamma\Delta H_{pp} . \qquad (8)$$

Using formula (8), the dependence of the magnetic relaxation time on the concentration of Zn^{2+} ions in the studied ferrites is calculated (see Fig. 8). Obviously, with increasing parameter x, relaxation time increases and leads to the decrease in the FMR line width. Small relaxation time (10^{-11} s) during the resonance energy absorption in magnesium-zinc samples can indicate that the spin-lattice and the spin-spin relaxations take place simultaneously [28].

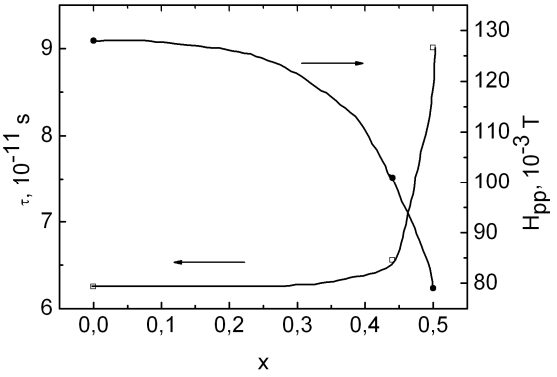

Fig. 8 – Dependence of the relaxation time and FMR line width on the diamagnetic substitution in $Mg_{1-x}Zn_xFe_2O_4$

We should note that during the FMR investigation of nickel-zinc ferrites, relaxation time was in the same range that for the magnesium-zinc samples. Increase in the relaxation time with increasing x implies that at low content of Zn^{2+} ions the spin-spin relaxation occurs faster that at high content.

4. CONCLUSIONS

The mechanisms and processes occurring during the synthesis of complex oxide systems by the sol-gel method with participation of auto-combustion have been studied based on the results of the performed investigations. It is established that in the production of ferrite powders, hydrolysis reaction takes place leading to the beginning of the sol formation. The neutralization process of the dispersion medium is carried out upon addition of ammonia water to the obtained colloidal solution resulting in the formation of ammonium nitrate. Drying of the sol leads to the increase in the concentration of the dispersion phase and beginning of the gel formation.

It is revealed that dry gel at 483 K catches fire because of the decomposition of ammonium nitrate and due

to the thermally induced oxidation-reduction interaction between the citrate and nitrate ions. A sufficient amount of energy is released in this case for the formation of the single-phase ferrite powders.

Investigation results of the obtained ferrite samples have shown that nano-sized particles of the powders are formed into aggregates during synthesis. Based on the data of the cation distribution of magnesium-zinc ferrites it is established that after passing of the auto-combustion process, cooling rate of particles corresponds to the quenching mode.

It is established that broadening of a magnetic sextuplet is observed with increasing number of Zn^{2+} ions in the composition of magnesium-zinc ferrites. Moreover, intensity of the central quadrupole doublet grows with increasing concentration of zinc ions. Rise of the paramagnetic doublet intensity is associated with a number of magnetic phenomena, namely, with the existence of superparamagnetic particles and magnetic phase with noncollinear arrangement of the magnetic moment vectors. Here, irrespective of the degree of substitution x, the presence of the magnetic-ordered phase is clearly observed. Increase in the Zn^{2+} content in the samples results in the decrease in the value of the effective magnetic fields in nuclei. It is obvious that the decrease in the magnetic fields induces weakening of the A-B interaction in the spinel structure.

The FMR line width decreases with increasing concentration of zinc in stoichiometric ferrites that is connected, as it turned out, with the decrease in the degree of reversibility of the spinel. This means that paramagnetic iron ions tend to occupy only one crystallographic position with increasing zinc concentration. In this case, antiferromagnetic interaction between iron ions located in the A- and B-sublattices weakens leading to the decrease in the value of ΔH_{pp}. The FMR-method confirms the results of the X-ray structural investigations of the cation distribution.

REFERENCES

1. L.I. Rabin, *Vysokochastotnyye feromagnetiki* (M.: Gos. izd. fiz-mat. literatury: 1960).
2. V.A. Bokov, *Fizika magnitnykh materialov* (SPb: Nevskiy dialekt: 2002).
3. Yu. Sitidze, Kh. Sato, *Ferrity* (M.: Mir: 1960).
4. T.Y. Byun, K.S. Hong, C.S. Yoon, C.K. Kim, *J. Magn. Magn. Mater.* **253**, 72 (2002).
5. Y. Yamamoto, H. Tanaka, T. Kawai, *J. Magn. Magn. Mater.* **261**, 263 (2003).
6. A.V. Kopayev, V.S. Bushkova, *Acta Phys. Polonica A* **117** No1, 30 (2010).
7. D. Bhalla, S.K. Aggarwal, G.P. Govil, I. Kakkar, *The Open Mater. Sci. J.* **4**, 26 (2010).
8. P. Zbigniew, *J. Eur. Ceramic Soc.* **24**, 1053 (2004).
9. B. Skołyszewska, *Physica C* **387**, 290 (2003).
10. A. Verma, T.C. Goel, R.G. Mendiratta, M.I. Alam, *Mater. Sci. Eng. B* **60**, 156 (1999).
11. B.K. Ostafiychuk, I.M. Gasyuk, O.V. Kopayev, *Phys. Chem. Solid State* **2** No2, 201 (2001).
12. M.N. Abdullah, A.N. Yusoff, *J. Alloy. Compd.* **233**, 129 (1996).
13. B.K. Ostafiychuk, I.M. Gasyuk, O.V. Kopaev, V.M. Nadutov, L.S. Yablon, *Phys. Chem. Solid State* **2** No3, 387 (2001).
14. B.K. Ostafiychuk, A.V. Kopayev, I.M. Gasyuk, *Functional Mater.* **6** No4, 686 (1999).
15. A.V. Kopayev, P.Y. Vyslobods'kyy, I.M. Hasyuk, *Visnyk Prykarpat's'koho universytetu. Seriya pryrodnycho-matematychnykh nauk* **1**, 119 (1994).
16. C. Upadhyay, H.C. Verma, S. Anand, *J. Appl. Phys.* **95** No10, 5746 (2004).
17. S. Dey, A. Roy, J. Ghose, R.N. Bhowmic, R. Ranganathan, *J. Appl. Phys.* **90**, 4138 (2001).
18. M. Kharinskaya, *Elektronika* **1**, 24 (2000).
19. O.V. Kopayev, I.Ya. Vylka, Pat. 36451 C01G49/00, C01G53/00, H01F1/00, Ukrayina, opubl. 27.10.2008.
20. V.S. Bushkova, V.V. Uhorchuk, *FKhTT* **12** No4, 1102 (2011).
21. Z. Yue, W. Guo, J. Zhou, Z. Gui, L. Li, *J. Magn. Magn. Mater.* **270**, 216 (2004).
22. V.S. Bushkova, Yu.M. Tafiychuk, I.Ya. Vylka, *Nanosystemy, nanomateriyaly, nanotekhnolohiyi* **10** No2, 297 (2012).
23. V.S. Bushkova, I.Ya. Vylka, *Metallofiz. Noveysh. Tekhnol.* **33**, 173 (2011).
24. A.V. Kopayev, B.K. Ostafiychuk, I.Y. Vylka, D.L. Zadnipryannyy, *Mat.-wiss. u. Werkstofftech* **40** No4, 255 (2009).
25. S. Hafner, *Metalloxyde mit Spinellstructur*, *Schweiz. miner. und petrogr. Mitt.* **40** No2, 207 (1960).
26. O.N.C. Uwakweh, R.P. Moyet, R. Mas, *J. Phys. Confer. Ser.* **217**, 012087 (2010).
27. V.I. Nikolayev, V.S. Rusakov, *Messbauerovskiye issledovaniya ferritov* (M.: Izd. Moskovskogo universiteta: 1985).
28. A.G. Gurevich, *Magnitnyy rezonans v ferritakh i antiferromagnetikakh* (M.: Nauka: 1973).
29. S. Krupichka, *Fizika ferritov i rodstvennykh im magnitnykh okislov* (M.: Mir: 1976).